

Article

Thermal Management of Diesel Engine Aftertreatment System Based on Ultra-Low Nitrogen Oxides Emission

Ke Sun ¹, Gecheng Zhang ¹, Zhengyong Wang ¹, Da Li ¹, Guoxiang Li ¹, Shuzhan Bai ^{1,*}, Chunjin Lin ^{2,*} and Hao Cheng ³

¹ School of Energy and Power Engineering, Shandong University, Jinan 250061, China; liguox@sdu.edu.cn (G.L.)

² Geotechnical and Structural Engineering Research Center, Shandong University, Jinan 250061, China

³ School of Aeronautic Science and Engineering, Beihang University, Beijing 100191, China

* Correspondence: baishuzhan@sdu.edu.cn (S.B.); linchunjin@sdu.edu.cn (C.L.)

Abstract: To achieve diesel engine ultra-low nitrogen oxide emission, light-off selective catalyst reduction (LO-SCR) has been suggested for better performance with lower exhaust temperature. An electric heater upstream of the exhaust aftertreatment system was applied to significantly decrease the NO_x emission at a low exhaust temperature. With a 7.2 kW electric heater coupled with LO-SCR, the NO_x emission during 200~500 s of the world harmonized transient cycle (WHTC) decreased from 282.6 ppm to 61.5 ppm, which is a decrease of 45%. Application of an upstream diesel oxidation catalyst (DOC) decreased the NO_x emission by 63% at the same interval at the cost of worse cold-start performance. The urea input was also adjusted to avoid NO_x emission during the latter part of the WHTC.

Keywords: diesel engine; aftertreatment; thermal management; SCR



Citation: Sun, K.; Zhang, G.; Wang, Z.; Li, D.; Li, G.; Bai, S.; Lin, C.; Cheng, H. Thermal Management of Diesel Engine Aftertreatment System Based on Ultra-Low Nitrogen Oxides Emission. *Appl. Sci.* **2024**, *14*, 237. <https://doi.org/10.3390/app14010237>

Academic Editor: Jun Cong Ge

Received: 12 November 2023

Revised: 7 December 2023

Accepted: 20 December 2023

Published: 27 December 2023



Copyright: © 2023 by the authors. Licensee MDPI, Basel, Switzerland. This article is an open access article distributed under the terms and conditions of the Creative Commons Attribution (CC BY) license (<https://creativecommons.org/licenses/by/4.0/>).

1. Introduction

Diesel engines have been widely used on various occasions because of their excellent thermal efficiency and reliability. However, nitrogen oxide (NO_x) emissions from diesel engines have an adverse effect on human beings and the environment [1], and regulations for diesel engine NO_x emission have been put forward by governing bodies all over the world [2]. According to Euro VI legislation, NO_x are restricted under 0.40 g/kW·h (steady-state testing) and 0.46 g/kW·h (transient-state testing), respectively [3]. Even so, the super ultra-low NO_x (ULN) emission standards for medium-duty vehicles, established by the California Air Resources Board, requires that the total emissions of nonmethane organic gases and NO_x are no more than 0.02 g/mile under the Heavy-Duty Federal Test Procedure (HD-FTP) [4]. This requires further alteration and improvement in NO_x emission control technologies.

Current legislation limitations already strictly require combining aftertreatment technologies. As the mainstream exhaust aftertreatment (EAT) technology route, the combination of a diesel oxidation catalyst (DOC) + a catalytic diesel particulate filter (CDPF) + selective catalytic reduction (SCR) + an ammonia slip catalyst (ASC) presents excellent performance on emissions control at the cost of limited decrease in thermal efficiency [5]. Even though the current method has already achieved above 95% NO_x conversion, the EAT system scheme still requires further adjustment and optimization in schemes and strategies for ULN emission regulation. Zavala et al. [4] proposed different aftertreatment configurations for ULN emission control, with light-off selective catalyst reduction (LO-SCR) applied close to the engine to take advantage of the higher exhaust temperatures.

SCR is the critical device in the EAT De-NO_x progress. The Cu-zeolite catalyst is a common choice to meet current regulations. Metkar et al. [6] studied the effects of the Fe-ZSM-5 and Cu-CHA catalysts on the NO_x reduction performance of NH₃, gave the

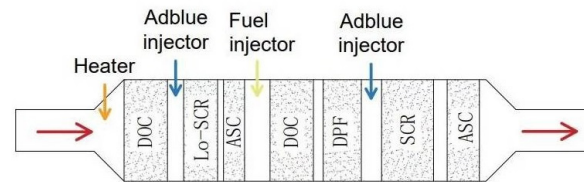
kinetic parameter values for Cu-CHA catalysts, and established a global kinetic model, which can better predict the conversion rate of NO_x and NH_3 . Mohan et al. [7] reviewed the performance of NH_3 -SCR using Cu-based catalysts in reducing NO_x at low temperatures and compared the ability of several Cu-based catalysts to reduce NO_x (standard SCR reaction) in different temperature ranges. Among them, Cu/SSZ is currently the most suitable catalyst for low-temperature reduction of NO_x , and the NO_x removal rate can reach 100% when the temperature is between 150 and 350 °C. When the temperature is lower than 150 °C, the NO_x reduction activity of Cu/SSZ drops sharply. Lei et al. [8] studied the effect of exhaust temperature on the efficiency of selective catalytic reduction (SCR) denitrification. Lei summarizes that the change in SCR denitrification efficiency generally includes three states based on exhaust gas temperature. In state I, the SCR carrier temperature is high and urea is injected, resulting in high NO_x conversion efficiency (>90%); state III is a cold-start condition with the lowest NO_x conversion efficiency (<50%). State II is a transitional stage involving ammonia storage. The NO_x conversion efficiency is linearly related to exhaust temperature and increases with increasing temperature; the slope of the NO_x conversion efficiency decreases with increasing exhaust temperature. Gholami et al. [9] reviewed different NO_x emission-reduction technologies and introduced the chemical reaction mechanism of NH_3 -SCR (standard SCR) under aerobic and anaerobic conditions. Xie et al. [10] conducted experimental research on the NO_x conversion efficiency and NH_3 leakage of three aftertreatment schemes by introducing SCR size strategies. Xie used postprocessing systems with different SCR lengths of the same SCR diameter and found that the nitrogen oxide emissions of the three SCR systems were similar, but the average NH_3 leakage varied greatly. As the SCR length decreased, the average NH_3 leakage increased. Ciardelli et al. [11] proposed a novel catalytic mechanism for the fast SCR reaction of NH_3 , NO, and NO_2 at low temperatures and supported a theoretical basis for fast SCR-related research. Yang et al. [12] studied the effect of fast SCR reaction on commercial SCR catalysts and found that fast SCR can apparently promote catalytic activity and decrease catalyst consumption and replacement frequency.

However, Cu-based catalysts may generate N_2O and have little capability to clarify it. Yao et al. [13] suggested reducing the amount of Cu in Cu-zeolite SCR to reduce N_2O generation without increasing NO_x emission. Kim et al. [14] examined the Fe-zeolite catalyst and achieved significant suppression of N_2O formation. Zhang and Yang analyzed the formation pathways of N_2O in a combined zeolite-supported SCR with both Fe and Cu catalysts. The later research of Sharp et al. also selected this method for better N_2O reduction [15].

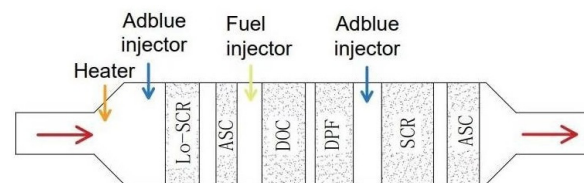
The DOC is applied to oxidize CO, HC, and other combustible emissions of diesel engines [16]. A DOC coupled with DPF or CDPF has been widely applied for particulate matter clarification [17]. The oxidization process within DOC also affects NO, which can benefit the passive regeneration in downstream CDPF [18] and SCR. As the EAT thermal management largely focused on the DOC, the exhaust temperature and constituents of NO_x , mainly NO and NO_2 , will also affect the NH_3 - NO_x reactions of downstream SCR [19]. Nova et al. [20] suggested that, compared to other NO_2/NO_x ratios, the efficiency of the SCR reaction can be promoted to the greatest extent when the NO_2/NO_x ratio reaches 50%. Based on the inherent characteristics of high NO emission (more than 90%) of diesel engines, a feasible solution to improve De- NO_x efficiency and decrease urea water solution consumption is increasing the SCR inlet NO/ NO_2 ratio to 1:1 [21]. Li et al. [22] proposed that the optimal ratio of NO_2 to NO_x in SCR may be 1:2, at which the nitrogen removal efficiency and the amount of N_2 generated are maximized, with relatively less N_2O produced. By increasing the ratio of NO_2 to NO_x , the NO content at the outlet gradually decreases, while the N_2 content first increases and then decreases and the N_2O content increases.

The relative location of the DOC, whether upstream (scheme A in Figure 1) or downstream (scheme B in Figure 1) of LO-SCR, also requires consideration. A DOC deployed upstream provides the possibility to partially oxidize NO into NO_2 and increase the propor-

tion of fast reactions. However, at lower exhaust temperatures, a higher NO_2 concentration will increase N_2O generation, [23], while, at higher exhaust temperatures, possible NO_2 surplus caused by an increased generation rate in the DOC will further hinder the $\text{NH}_3\text{--NO}_x$ reactions in SCR. Another problem for the upstream DOC scheme is its effect on exhaust temperature; at cold start conditions, the cold DOC upstream will delay the catalyst temperature increase of LO-SCR [4].



Scheme A. The DOC is upstream of LO-SCR



Scheme B. The DOC is downstream of LO-SCR

Figure 1. Related exhaust aftertreatment system schemes.

Therefore, to achieve ULN emission control at mid to low load, the EAT thermal management strategy requires detailed analysis. This work focused on the $\text{NH}_3\text{--NO}_x$ reactions in LO-SCR and related thermal management strategy optimization. Two major aspects were evaluated in this work: the effect of thermal management strategy on exhaust parameters before SCR and the effect of thermal management strategy on LO-SCR performance at ULN emission control. The former was analyzed through a diesel engine EAT bench test, focused on exhaust temperature increase with an electric heater and NO oxidation in a DOC. The latter was evaluated through simulation, mainly for the comparison of different EAT system schemes, and the final Lo-SCR performance with the optimized thermal management strategy. This paper can be a reference for ULN emission control at mid- to low-load working conditions.

2. Method

2.1. EAT System Experiments

2.1.1. Test Bench Structure

The experiments were performed on a certain six-cylinder in-line China VI engine that was equipped with a high-pressure common rail system and a VGT with an intercooler. The EAT system test bench is given in Figure 2, and Figure 3 is the scheme of the test bench. The parameters of the test engine are listed in Table 1. The EAT system, focused on DOC and LO-SCR, was arranged for this research. The details of the measurement equipment are listed in Table 2. NO_x and O_2 were measured by chemiluminescence detection (CLD) and paramagnetic detection (PMD), respectively.



Figure 2. EAT system test bench.

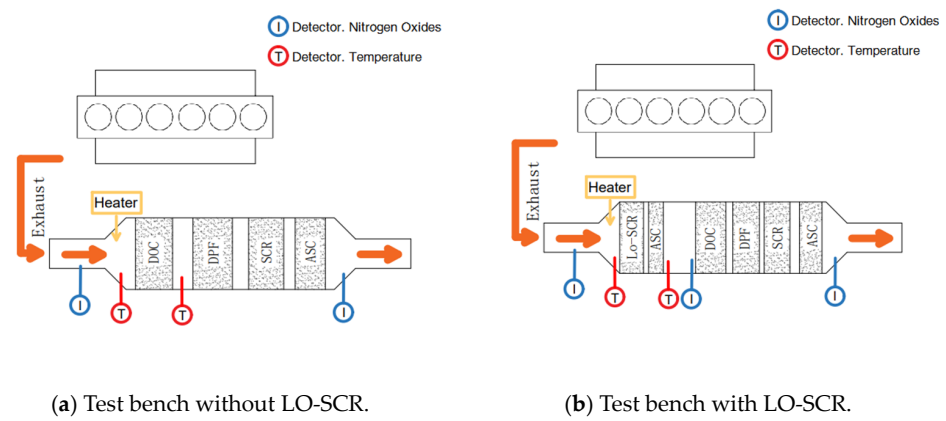


Figure 3. Test bench structure.

Table 1. Engine parameters.

Project	Specification
Engine type	6-cylinder in-line/inter-cooling
Bore \times Stroke/mm \times mm	117 \times 135
Displacement/L	8.7
Rated power/kW	280
Rated speed/r/min	2100
Idle speed/r/min	700
EGR rate	0
Turbocharger	VGT

Table 2. Specification of measurement equipment.

Equipment	Model	Measuring Principle	Accuracy of Measurement
Electric dynamometer	INDYS66JD	-	Speed: ± 1 r/min Torque: $\pm 0.1\%$ FS
Exhaust gas analyser	I60	NO _x : CLD O ₂ : PMD	1 ppmvol 0.01%vol
Opacimeter	483	Photoacoustic method	5 μ g
Fuel consumption meter	FC2212L	-	$\pm 0.2\%$
Thermocouple	RTD100	-	1 $^{\circ}$ C

2.1.2. Cycle Experiments

To investigate the NO_x emission and other exhaust parameters during cold-start and mid- to low-load working conditions, a diesel engine emission experiment was carried out using the World Harmonized Transient Cycle (WHTC). The exhaust parameter before and after LO-SCR during cold-start WHTC was recorded for simulation. The NO oxidization capability of DOC was also investigated during the cycle experiment.

This paper was focused on reducing NO_x emission at mid- to low-load working points, where exhaust temperature is relatively low. Therefore, the traditional thermal management of throttle valve opening adjustment and postinjection is insufficient in this case. A separate heater is placed before DOC, heating the exhaust before entering the EAT system, to effectively increase the catalyst temperature at a lower load. Temperature variations of the LO-SCR catalyst (at the inlet) before and after thermal management are given in Figure 4. After the application of an electrical heater, the SCR catalyst temperature increased by 25.75°C on average during 0~500 s of WHTC.

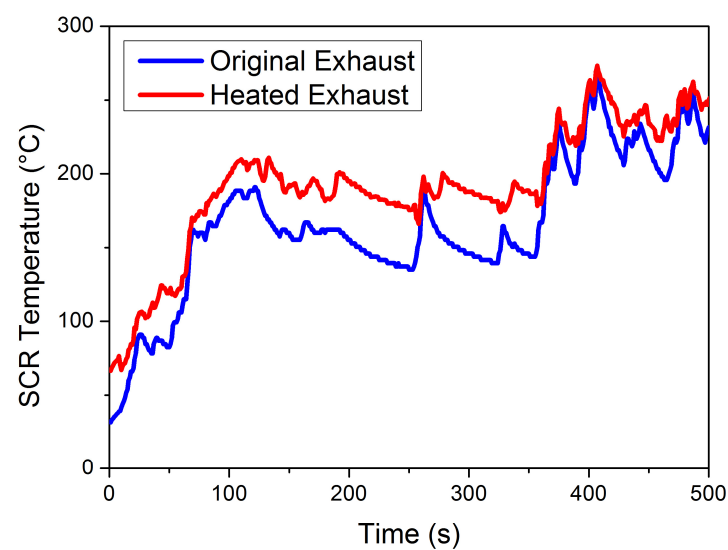


Figure 4. Heated SCR catalyst temperature (at the inlet) during WHTC.

The altered catalyst temperature will be taken into the simulation model to fully simulate the effect of electrical heating on the EAT system with ULN emission. It is possible to place the DOC before LO-SCR to partially oxidize NO into NO_2 and increase the proportion of fast reaction in SCR. For scheme A in Figure 1, the temperature input of the upstream DOC is taken from the LO-SCR inlet during the thermal management bench test, while the LO-SCR inlet parameter will be determined by the upstream DOC.

2.2. Modeling

2.2.1. Chemical Model

1. De- NO_x Reactions inside SCR

The NO_x conversion of diesel engine exhaust mostly occurred in SCR, chemical reactions inside SCR are listed in Table 3 [5], and the three main reactions in SCR are R4 (standard reaction), R5 (fast reaction), and R6 (slow reaction). The reaction rate of a fast reaction can be 17 times higher than a standard reaction [13]; optimizing the ratio between NO and NO_2 towards a larger proportion of fast reactions can thus effectively improve the NH_3 - NO_x reaction rate. The slow reaction of R6 is neglectable in practical simulation models. Still, R6 is taken into consideration during model construction. It should be mentioned that NH_3 may be oxidized by oxygen, as represented in R2. The NH_3 consumption caused by the NH_3 - O_2 reaction, or ammonia chemical loss, increases at

higher exhaust temperatures, which requires further consideration after the application of electrical heating.

Table 3. Related SCR reactions.

No.	Reactions $k^f = AT^b \exp(-E/RT)$	A	b	E (kJ/mol)
R1	$\text{NH}_3 + \text{S} \rightarrow \text{NH}_3\text{-S}$	6.68×10^7	0	0
R2	$2\text{NH}_3\text{-S} + 1.5\text{O}_2 \rightarrow \text{N}_2 + 3\text{H}_2\text{O} + 2\text{S}$	5.56×10^{16}	0	178.8
R3	$\text{NO} + 0.5\text{O}_2 \leftrightarrow \text{NO}_2$	5.1×10^7	0	56
R4	$4\text{NH}_3 + 4\text{NO} + \text{O}_2 \rightarrow 4\text{N}_2 + 6\text{H}_2\text{O}$	7.08×10^{13}	0	89.1
R5	$2\text{NH}_3 + \text{NO}_2 + \text{NO} \rightarrow 2\text{N}_2 + 3\text{H}_2\text{O}$	1.0×10^{18}	0	77.1
R6	$4\text{NH}_3 + 3\text{NO}_2 \rightarrow 7/2\text{N}_2 + 6\text{H}_2\text{O}$	1.96×10^{17}	0	136.3
R7	$2\text{NH}_3\text{-S} + \text{NO}_2 \rightarrow \text{N}_2 + \text{NH}_4\text{NO}_3 + \text{H}_2\text{O} + 2\text{S}$	2.28×10^8	0	43
R8	$\text{NH}_4\text{NO}_3 \rightarrow \text{N}_2\text{O} + 2\text{H}_2\text{O}$	1.25×10^8	0	41.5

2. Reactions inside DOC

Reactions inside DOC are summarized as R9~R16 in Table 4, referred to by researchers of Hsieh et al. [24].

Table 4. DOC reactions.

No.	Reactions $k^f = AT^b \exp(-E/RT)$	A	b	E (kJ/mol)
R9	$\text{NO} + 0.5\text{O}_2 \leftrightarrow \text{NO}_2$	5.1×10^7	0	56
R10	$\text{NO} + \text{CO} \rightarrow \text{CO}_2 + 0.5\text{N}_2$	2.857×10^9	0	52.374
R11	$9\text{NO} + 1\text{C}_3\text{H}_6 \rightarrow 3\text{CO}_2 + 4.5\text{N}_2 + 3\text{H}_2\text{O}$	2.994×10^{11}	0	80.063
R12	$\text{NO} + \text{H}_2 \rightarrow \text{H}_2\text{O} + 0.5\text{N}_2$	7.88×10^{10}	0	69.237
R13	$\text{CO} + 0.5\text{O}_2 \rightarrow \text{CO}_2$	1.183×10^{12}	0	81.33
R14	$\text{H}_2 + 0.5\text{O}_2 \leftrightarrow \text{H}_2\text{O}$	9.83×10^4	0	15.31
R15	$\text{C}_3\text{H}_6 + 4.5\text{O}_2 \rightarrow 3\text{H}_2\text{O} + 3\text{CO}_2$	1.566×10^{19}	0	159.4
R16	$\text{H}_2\text{O} + \text{CO} \leftrightarrow \text{H}_2 + \text{CO}_2$	1.8×10^5	0	56.72

Reactions between NO and CO, H₂, and unburned HC consume limited NO, while NO₂ generated through R9 has a significantly greater effect on the SCR downstream. Increased NO₂ at SCR inlet has both pros and cons on the NH₃-NO_x reaction rate. Limited NO₂ in SCR will mostly be consumed in a fast reaction; the high reaction rate can improve the conversion rate, especially at lower temperatures with low reaction rates. However, if NO is completely clarified before NO₂, the remaining NO₂ will be difficult to clarify with only a slow reaction. In addition, R7 and R8 together will generate N₂O, which is extremely difficult to clarify with Cu-zeolite SCR [20], and excess NO₂ may increase the possibility of R7 happening, especially at lower temperatures [11]. The NO oxidation in DOC shall be taken into consideration.

2.2.2. EAT System Model

Modeling of the EAT system is focused on LO-SCR. The LO-SCR model was constructed in GT-Power(GT-SUITE version 2021), as shown in Figure 5. Related SCR parameters are given in Table 5.

Table 5. EAT system parameters.

	DOC	DPF	SCR	ASC
Volume (L)	2.17	3.62	2.90	2.90
Diameter (mm)	190.5	190.5	190.5	190.5
Length (mm)	76.2	127	101.6	101.6

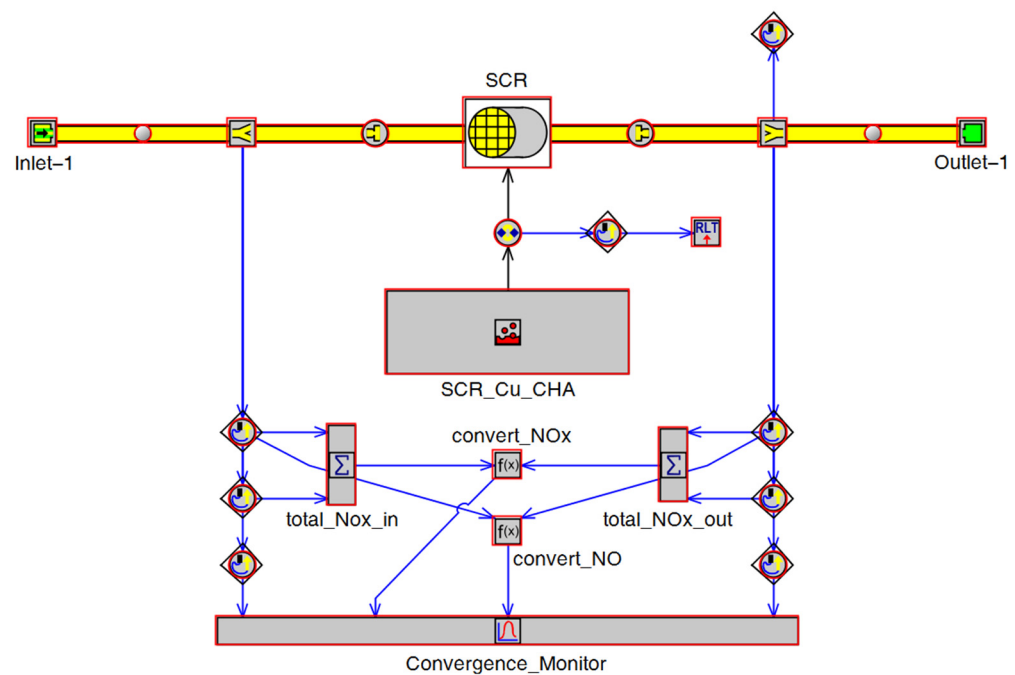


Figure 5. SCR simulation model.

3. Result and Analysis

3.1. SCR Reaction at Steady Working Point

At a certain working point taken from the world harmonized steady-state cycle (WHSC), the reaction within SCR at exhaust temperatures between 200 °C and 500 °C is shown in Figure 6a, where exhaust mass flow and inlet NO_x remain constant. At lower exhaust temperatures, the NH_3 – NO_x reaction rate is hindered by the low temperature, as exhaust temperature increases, the NO_x conversion rate gradually increases from 87.07% at 200 °C to 97.81% at 260 °C. After peaking at 260 °C, the NO_x conversion rate decreases with a further increase in the exhaust temperature. With the ammonia–nitrogen ratio fixed at 1:1, a higher proportion of ammonia reacting with oxygen will hinder the reaction of ammonia with nitrogen oxides; the ratio of unclarified nitrogen oxides is almost equal to ammonia consumed by the NH_3 – O_2 reaction. It should be pointed out that this is not the case in practical Cu-zeolite SCR reactions, as the ammonia storage generally provides sufficient ammonia.

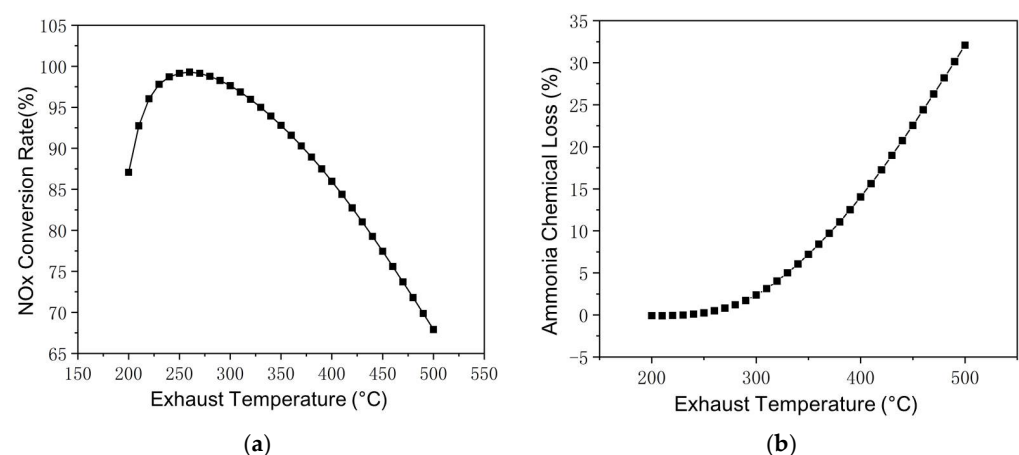


Figure 6. Reactions in SCR at different exhaust temperatures. (a) Changes of NO_x Conversion Rate with Exhaust Temperature. (b) Changes of Ammonia Chemical Loss with Exhaust Temperature.

Within the exhaust temperature range selected in Figure 6, the reaction between ammonia and oxygen also increases with increasing temperature, as shown in Figure 6b. At an exhaust temperature below 250 °C, the ammonia–oxygen reaction consumes less than 0.1% NH_3 input and the $\text{NH}_3\text{--O}_2$ reaction is neglectable. As the exhaust temperature increases to over 300 °C, the $\text{NH}_3\text{--O}_2$ reaction rate begins to increase significantly, from 2.37% at 300 °C to 7.2% at 350 °C, 14.03% at 400 °C, and 32.09% at 500 °C. For road vehicles, the diesel engine is less likely to operate constantly at a high exhaust temperature range. Even so, with SCR catalyst temperature above 250 °C, the loss still requires consideration.

The effect of exhaust mass flow is shown in Figure 7, with other parameters remaining constant. It should be noted that the NO_x inlet in PPM is fixed, thus increasing exhaust mass flow, which increases the NO_x quantity in SCR. This is the main factor that affects the NO_x conversion rate at different mass flow rates. Increasing the mass flow by 40% reduces the NO_x conversion rate to 82.1%, while decreasing it by 40% improves the conversion rate to 97.6%. The effect of exhaust flow change on the ammonia–oxygen reaction is also significant and the $\text{NH}_3\text{--O}_2$ reaction rate decreases with the increase in exhaust mass flow and the ammonia chemical loss decreases from 0.75% to 0.46% between -40% and $+40\%$. The effect of mass flow itself is less significant than exhaust temperature and SCR carrier length.

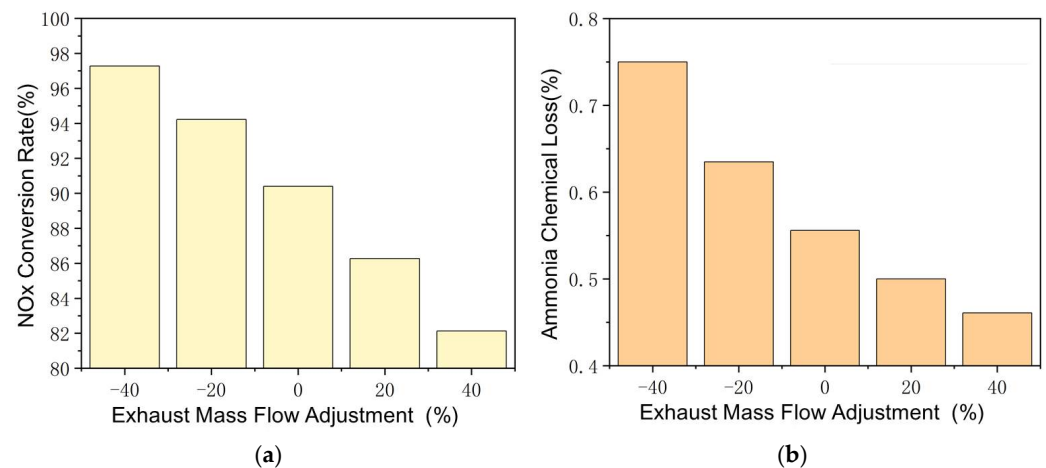


Figure 7. Reactions in SCR at different exhaust mass flows. (a) Changes of NO_x Conversion Rate with Exhaust Mass Flow Adjustment. (b) Changes of Ammonia Chemical Loss with Exhaust Mass Flow Adjustment.

The effect of SCR carrier length is shown in Figure 8, with other parameters also remaining constant. Longer carrier length means a larger area and longer time for catalyzed reactions, which improves the $\text{NH}_3\text{--NO}_x$ reaction rate and NO_x conversion rate, even at lower exhaust temperatures. The conversion rate of NO_x increases from 92.1% to 98.2% as the SCR carrier length increases from 100 mm to 200 mm. The $\text{NH}_3\text{--O}_2$ reaction rate is also significantly affected by the change in carrier length. At lower exhaust temperatures, as the carrier length increases from 100 mm to 200 mm, the ammonia chemical loss increases from 0.55% to 0.83%. Since the ammonia–nitrogen ratio is fixed at 1:1, the increase in the $\text{NH}_3\text{--O}_2$ reaction rate hinders the $\text{NH}_3\text{--NO}_x$ reaction at longer carrier length. It is necessary to further improve the $\text{NH}_3\text{--NO}_x$ reaction rate, and the ammonia–nitrogen ratio in steady-state working points should be greater than 1. It should be noted that a longer SCR carrier can store more ammonia, which may cause larger ammonia leakage at transient working points.

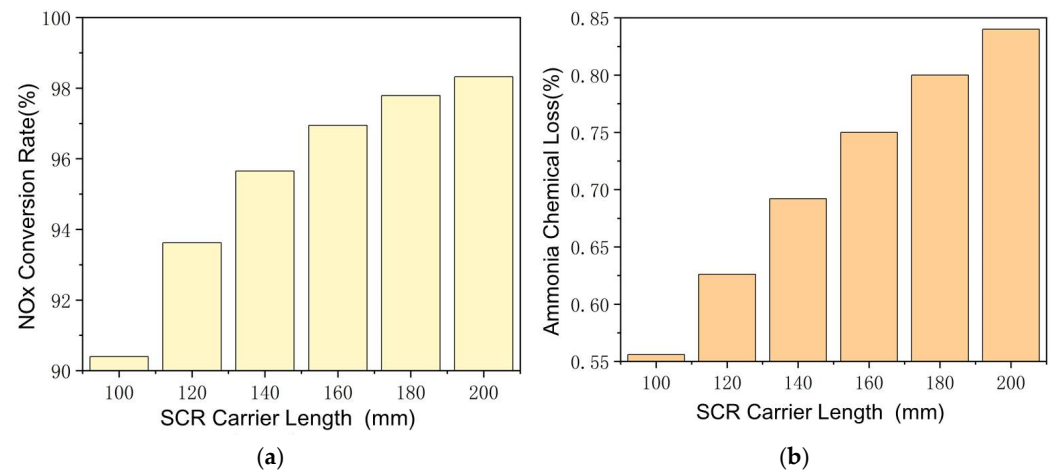


Figure 8. Reactions in SCR at different carrier lengths. (a) Changes of NO_x Conversion Rate with SCR Carrier Length. (b) Changes of Ammonia Chemical Loss with SCR Carrier Length.

The effect of DOC on the NO_x conversion rate after thermal management should also be emphasized. Nitrogen oxides generated during combustion are mostly NO, and the DOC at SCR upstream can partially oxidize NO into NO₂. The NO_x conversion rate at different SCR inlet NO_x compositions (NO and NO₂ only; other possible nitrogen oxides were neglected) is given in Figure 9, with the exhaust parameter and ammonia input remaining constant. The NO_x concentration at the SCR inlet is higher than in Figures 6–8 for better comparison. The effect of exhaust temperature at this working point is still generally positive for NO_x conversion, while the effect of NO oxidization depends on actual SCR temperature. At lower temperatures with lower catalyst activity, a higher NO₂ proportion can increase the proportion of fast reactions. With exhaust temperature at 200 °C, the NO_x conversion rate of 40% NO₂ (60% NO) is 77.57%, significantly higher than the 49.01% of 100% NO; at 250 °C, the difference caused by NO₂ is limited. However, the consumption rate of NO is higher than NO₂; thus, NO may be completely clarified before complete NO₂ conversion, especially at higher temperatures, and NH₃–NO₂ reaction rate is significantly low and N₂O is likely to be generated during this process. With 40% NO₂ at the inlet and exhaust temperature at 300 °C, the NO_x emission at the SCR outlet increased to 7.15%, while, with 100% NO, the emission is only 3.38%. It should be noted that the NO_x at the SCR inlet in Figures 6–8 is completely NO. The effect of DOC after thermal management requires further consideration.

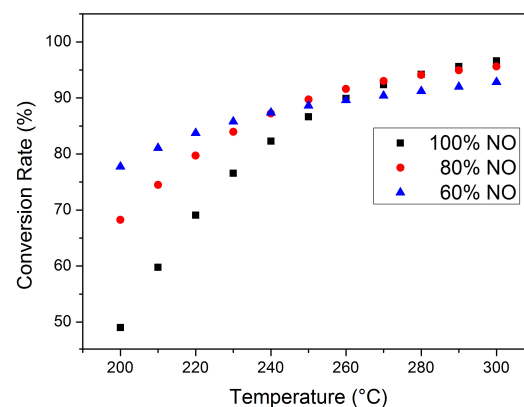


Figure 9. Total NO_x conversion rate at different inlet conditions.

In summary, the low exhaust temperature at lower load working points will inevitably decrease the SCR catalyst activity. To improve the NH₃–NO_x reaction rate, a higher exhaust temperature is required and a proper NO/NO₂ ratio may also improve the conversion [19].

Methods that improve the reaction between ammonia and nitrogen oxides will also improve the ammonia–oxygen reaction. Thermal management is required to further decrease NO_x emission, and the increase in ammonia chemical loss should also be taken into consideration [4].

3.2. SCR Reaction at Transient Cycle

The steady-state condition analysis in the previous section investigated the effect of various factors. Under transient working conditions, the exhaust temperature and mass flow rate change frequently and the temperature of the SCR carrier will also be affected, thereby affecting the NH_3 – NO_x reaction. Therefore, before analyzing thermal management methods to further decrease NO_x emission, it is necessary to analyze the SCR NO_x conversion capacity at a transient cycle.

The WHTC cycle test is relatively close to the actual driving cycle and the engine operates under frequent varying conditions. The NO_x emission of a conventional EAT system under the WHTC cycle without thermal management intervention is shown in Figure 10. High NO_x emission levels mainly occur in the first third of the entire cycle, while the emission at the latter part of the cycle remains low. The results of NO_x emission before 200 s are not taken into consideration in Figure 10, as thermal management is inevitably required to reduce NO_x emission under cold starting conditions. In Figure 10a, compared to the 500~1800 s range (Figure 10b–d), the NO_x emission is higher in the 200~500 s range (indicated by the blue line in Figure 10a). The peak NO_x emission occurs at 361 s, with a value of 465.4 ppm. The average conversion rate of NO_x at 200~500 s is only 62.58%, which may be due to the SCR carrier not having been raised to the appropriate temperature. Even with the NO_x emissions of the starting condition, the NO_x emissions of 200~500 s account for 39.21% of the total emissions.

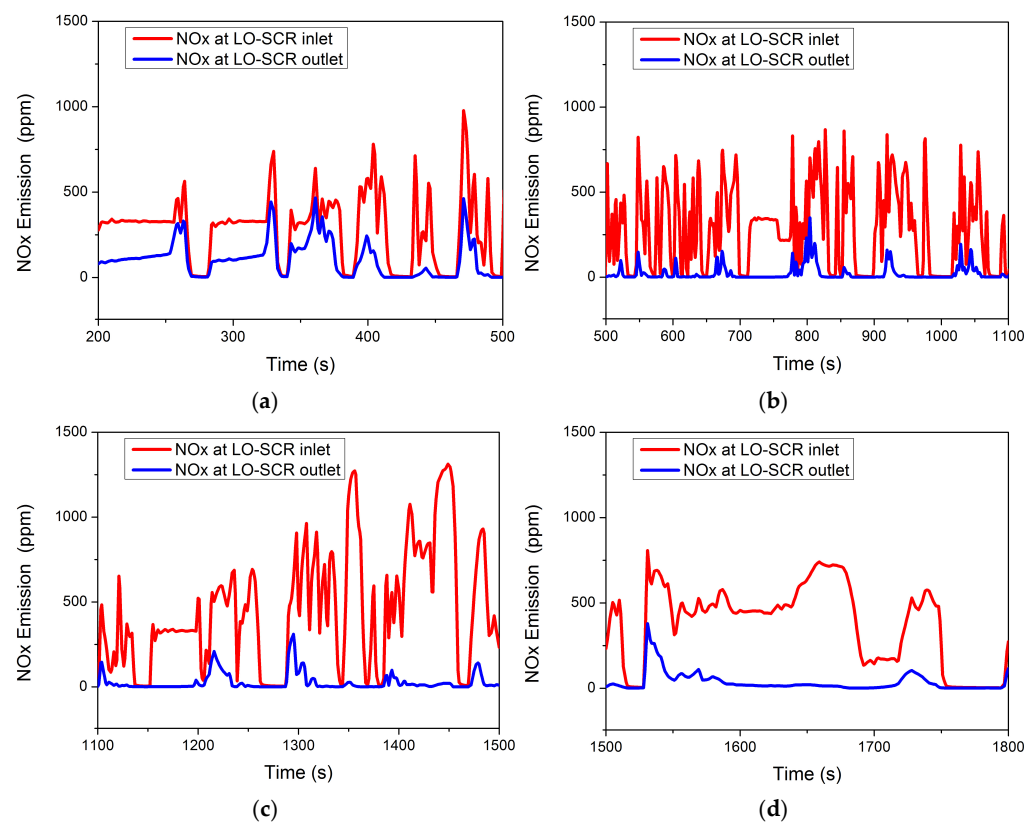


Figure 10. NO_x at LO-SCR inlet and outlet during WHTC cycle at (a) 200~500 s, (b) 500~1200 s, (c) 1200~1500 s, and (d) 1500~1800 s.

In Figure 10b, the NO_x content in the engine exhaust gas does not change significantly compared to before (indicated by the red broken line in Figure 10b). The average NO_x content is 282.6 ppm in the interval of 500~1100 s, while it is 280.2 ppm in the interval of 200~500 s. However, due to the increase in SCR carrier temperature, the NO_x emission decreases significantly. In the interval of 500~1100 s, the peak NO_x emission decreases to 349.2 ppm, occurring at 801 s, and the average conversion efficiency of NO_x increases to 92.48%.

In the interval of 1100~1500 s, as shown in Figure 10c, the NO_x content in the engine exhaust increases compared to the previous period, and the average NO_x content rises to 457.8 ppm. At the same time, due to the high temperature of the SCR carrier, the NO_x emission does not change significantly compared to the interval of 500~1100 s, which further increases the average NO_x conversion rate to 93.96%.

In the interval of 1500~1800 s, as shown in Figure 10d, the average content of NO_x in the engine exhaust gas decreases to 361.6 ppm; except for a few operating points where the NO_x emission changes significantly, the overall trend is smooth and the average conversion rate of NO_x is 90.01%. The average NO_x emission level in the first 500 s is 260 ppm, while the average NO_x emission from 500~1800 s is 10.5 ppm.

Under the WHTC cycle, there are more low-temperature conditions and more nitrogen oxide emissions. For the SCR system, the high-efficiency window of the catalyst is mainly 250~400 °C, so the catalytic conversion efficiency of the catalyst is affected under the condition of low exhaust temperature, resulting in the NO_x not being efficiently clarified. The high NO_x emissions in the first 500 s are mainly due to the low SCR carrier temperature, which only improved after higher exhaust temperature at the latter part of the cycle increased catalyst temperature to higher NO_x conversion capability. Therefore, the key to further improving the purification capacity under SCR variable working conditions and achieving ultra-low nitrogen emissions lies in mid- to low-load working conditions, and thermal management methods should also focus on this period, as suggested by the experimental investigation of Zavala et al. [4] and Sharp et al. [13].

3.3. Effect of DOC on SCR

The NO – NO_2 conversion rate within DOC at different exhaust temperatures and mass flows is given in Figure 11. When the exhaust temperature exceeds 425 °C, the conversion rate does not change significantly with the exhaust flow, while gradually decreasing with the increase in the exhaust temperature. Under medium load working points (in the range of 325 °C~425 °C), the exhaust mass flow has a significant effect on the NO_x conversion rate in DOC, and the variety of conversion rates is limited at higher exhaust mass flow. The effect of exhaust temperature on NO – NO_2 conversion rate is simple and significant. The high conversion rate mainly occurred between 350 °C and 400 °C, with medium to low exhaust flow rate from 300 kg/h to 525 kg/h. The highest conversion rate among all selected operating conditions is about 39.5%; the corresponding exhaust temperature and exhaust mass flow rate are 386 °C and 336.6 kg/h, respectively. It should be noted that the temperature is also within the optimistic temperature range of the SCR [17].

Figure 12 shows the NO_x conversion rates at three different EAT system schemes of the working points under low- to medium-load conditions of the engine. Exhaust temperature is increased through exhaust electric heating, with or without upstream DOC, which is reflected in the figure as the NO_x conversion efficiency at all three operating points being at a high level. At steady state and higher carrier temperature, the NO_2 generated in DOC still increases the proportion of fast reaction in SCR and improves the conversion rate of NO_x , which makes the NO_x conversion efficiency of the scheme involving upstream DOC slightly higher than the other two schemes at the three operating points. Under three working conditions, the NO_x emissions of the EAT system with upstream DOC decreases by 18.69%, 9.61%, and 14.15% compared to the conventional arrangement, although the NO_x conversion efficiency increases to a limited extent compared to the other two EAT systems without upstream DOC. It should be also noted that, at cold start conditions, an

upstream DOC will consume the heat of the exhaust and delay the catalyst temperature increase of LO-SCR and the effect on the cycle NO_x emission may be negative.

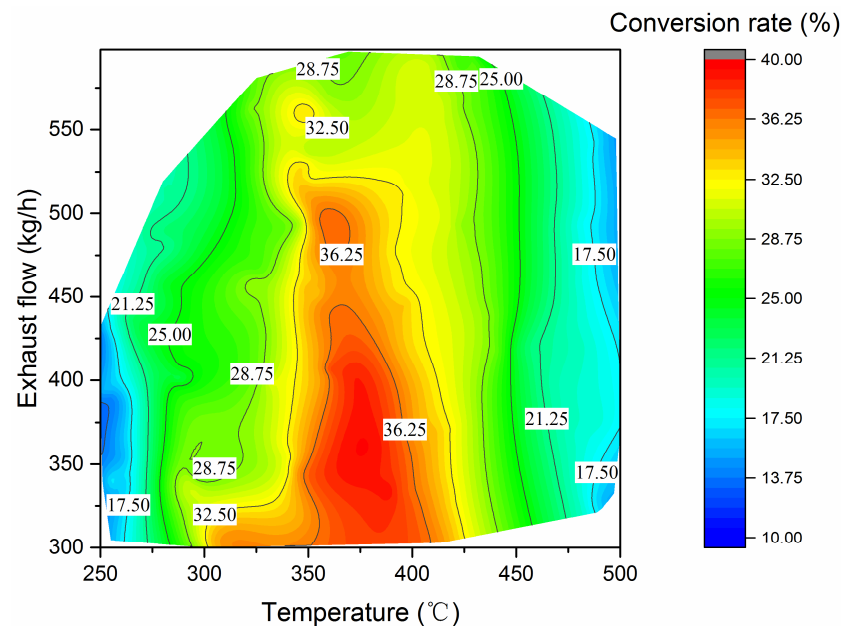


Figure 11. DOC NO_2 conversion rate.

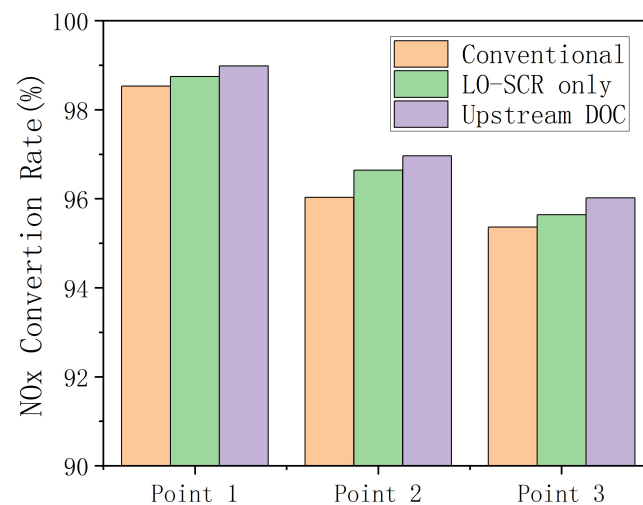


Figure 12. NO_x Conversion rate with different EAT system schemes.

4. Discussion

To effectively reduce NO_x emission at mid- to low-load working points, an electric heater was applied at SCR upstream. During the entire WHTC bench test, the exhaust was heated before entering the EAT system to improve the activity of the SCR catalyst at a lower exhaust temperature. The simulation result is shown in Figure 13. Increased temperature has improved the activity of cold-start SCR catalyst, and the effect of thermal management on NO_x emission is significant. During 200~500 s of WHTC test, after electrical heating, the average NO_x emission of the LO-SCR system is 61.5 ppm, a reduction of 45% compared to the value without electrical heating before. The effect of upstream DOC is also moderately positive, as the NO_x emission decreased by 63%, reaching 41.9 ppm. However, the effect of DOC will inevitably hinder the temperature increase of LO-SCR during the early stage of cold start. With higher exhaust temperature, the DOC before LO-SCR may generate NO_2 in a larger proportion, which will increase the possibility of N_2O generation. The moderate positive effect is insufficient to compromise these two concerns.

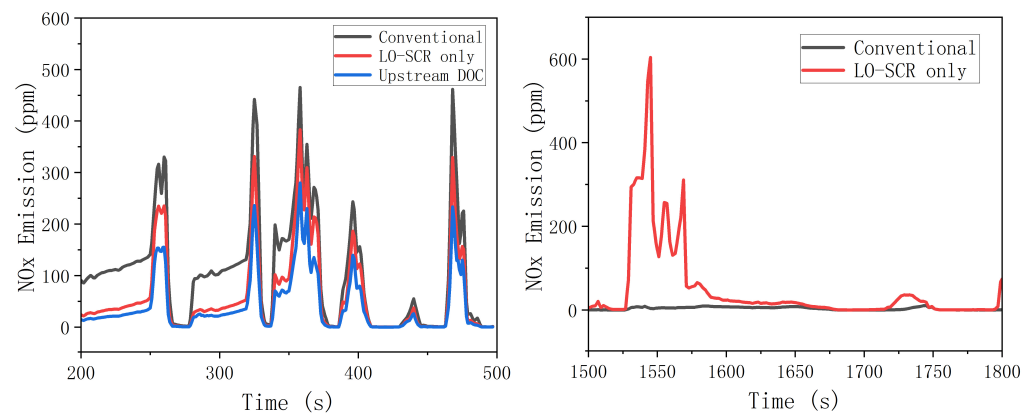


Figure 13. Effect of thermal management on NO_x conversion.

From 1500 to 1800 s, there was a significant difference in nitrogen oxide emissions between the EAT system with LO-SCR and the conventional arrangement system of 1500~1600 s. The increase in average exhaust temperature caused by thermal management increases the reaction rate between ammonia and oxygen, resulting in the increase in the ammonia chemical loss. If the urea input is not adjusted after thermal management, the ammonia storage is insufficient at 1500 s, which, in turn, leads to significant NO_x emission. The problem can be largely avoided by proper urea input adjustment.

5. Conclusions

To further decrease the nitrogen oxide emission of diesel engines, electrical heating is applied for better EAT system performance at mid- to low working points. The effect of exhaust parameter and DOC on NO_x conversion is investigated to further decrease the NO_x emission during the cold-start WHTC cycle.

1. At lower exhaust temperatures, the NH₃–NO_x reactions were hindered by the low temperature, which is consistent with the article mentioned in [8]. As exhaust temperature increases, the NO_x conversion rate gradually increases from 87.07% at 200 °C to 97.81% at 260 °C. Longer SCR carriers can also increase the NH₃–NO_x reaction rate at steady working points at the cost of higher capital cost and ammonia chemical loss, as mentioned in [10].
2. A separate LO-SCR coupled with an upstream electrical heater can effectively increase the NO_x conversion rate at lower exhaust temperatures. With a 7.2 kW electrical heater, the NO_x emission at the LO-SCR outlet decreased by 45% during the 200~500 s of the WHTC cycle.
3. The effect of DOC on the NH₃–NO_x reactions is twofold. At lower working points, partially oxidized NO into NO₂ increases the proportion of fast reaction in LO-SCR, while, at higher load working points, the high NO₂ proportion may increase N₂O generation and the proportion of slow reaction, similar to those mentioned in [21,22]. The upstream DOC decreased the LO-SCR outlet NO_x emission by 63% during the 200~500 s of the WHTC cycle at the cost of worse cold-start performance and higher N₂O emission.
4. The application of thermal management increased the average exhaust temperature, which increased the NH₃–O₂ reaction rate in SCR. The urea input shall be adjusted properly to avoid NO_x emission during the latter part of WHTC, as mentioned in [10].

Author Contributions: Conceptualization, K.S. and S.B.; methodology, K.S. and D.L.; software, Z.W.; validation, Z.W. and D.L.; formal analysis, D.L. and G.Z.; investigation, K.S., D.L. and G.Z.; resources, S.B. and C.L.; data curation, K.S. and G.Z.; writing—original draft preparation, K.S., Z.W. and D.L.; writing—review and editing, D.L., G.Z. and H.C.; visualization, G.Z. and Z.W.; supervision, G.L., S.B. and C.L.; project administration, K.S.; funding acquisition, G.L. and S.B. All authors have read and agreed to the published version of the manuscript.

Funding: This research was funded by Construction Machinery Intelligent Equipment Innovation and Entrepreneurship Community of Shandong, China (grant numbers GTT2021105), Department of Science & Technology of Shandong Province, China (grant numbers 2021TSGC1334), Asset & Laboratory Management Department of Shandong University, China (grant numbers sy20232305), and the Undergraduate School of Shandong University, China (grant numbers 2022Y155).

Institutional Review Board Statement: Institutional review is not applicable as the paper did not involve humans or animals.

Informed Consent Statement: Informed consent is not applicable as the paper did not involve humans.

Data Availability Statement: All data and models used in the study appear in the submitted article.

Acknowledgments: We appreciate the editors and reviewers for their constructive and detailed critiques that contributed to the quality of this paper, and all individuals have confirmed this acknowledgment.

Conflicts of Interest: The authors declare no conflict of interest.

Nomenclature

A	Pre-exponential factor
b	Positive constants
E (kJ/mol)	Activation energy
LO-SCR	Light-Off Selective Catalyst Reduction
NO_x	Nitrogen Oxides
HC	Hydrocarbon
WHTC	World Harmonized Transient Cycle
WHSC	World Harmonized Stationary Cycle
DOC	Diesel Oxidation Catalyst
EAT	Exhaust Aftertreatment
CDPF	Catalytic Diesel Particulate Filter
SCR	Selective Catalytic Reduction
ASC	Ammonia Slip Catalyst
VGT	Variable Geometry Turbocharger
ULN	Ultra-Low Nitrogen Oxides
CLD	Chemiluminescence Detector
PMD	Paramagnetic Detector

References

1. Lelieveld, J.; Evan, J.S.; Fnais, M.; Giannadaki, D.; Pozzer, A. The contribution of outdoor air pollution sources to premature mortality on a global scale. *Nature* **2015**, *525*, 367–371. [\[CrossRef\]](#) [\[PubMed\]](#)
2. Johnson, T.; Joshi, A. Review of Vehicle Engine Efficiency and Emissions. *SAE Int. J. Engines* **2018**, *11*, 1307–1330. [\[CrossRef\]](#)
3. Hooftman, N.; Messagie, M.; Van Mierlo, J.; Coosemans, T. A review of the European passenger car regulations—Real driving emissions vs local air quality. *Renew. Sustain. Energy Rev.* **2018**, *86*, 1–21. [\[CrossRef\]](#)
4. Zavala, B.; Sharp, C.; Neely, G.; Rao, S. CARB Low NO_x Stage 3 Program—Aftertreatment Evaluation and Down Selection; No. 2020-01-1402; SAE Technical Paper: Warrendale, PA, USA, 2020. [\[CrossRef\]](#)
5. Pan, Y.J.; Shen, B.X.; Liu, L.J.; Yao, Y.; Gao, H.P.; Liang, C.; Xu, H.J. Develop high efficient of NH_3 -SCR catalysts with wide temperature range by ball-milled method. *Fuel* **2020**, *282*, 118834. [\[CrossRef\]](#)
6. Metkar, P.S.; Harold, M.P.; Balakotaiah, V. Experimental and kinetic modeling study of NH_3 -SCR of NO_x on Fe-ZSM-5, Cu-chabazite and combined Fe- and Cu-zeolite monolithic catalysts. *Chem. Eng. Sci.* **2013**, *87*, 51–66. [\[CrossRef\]](#)
7. Mohan, S.; Dinesha, P.; Kumar, S. NO_x reduction behaviour in copper zeolite catalysts for ammonia SCR systems: A review. *Chem. Eng. J.* **2020**, *384*, 123253. [\[CrossRef\]](#)
8. Lei, Y.; Liu, C.; Guo, D.; Yang, J.; Qiu, T.; Peng, G. Real-Time Evaluation Method of Heavy-Duty Diesel Vehicle SCR System Based on Ammonia Storage Characteristics in Real-Road Driving Emission Test. *Appl. Sci.* **2022**, *12*, 11197. [\[CrossRef\]](#)
9. Gholami, F.; Tomas, M.; Gholami, Z.; Vakili, M. Technologies for the nitrogen oxides reduction from flue gas: A review. *Sci. Total Environ.* **2020**, *714*, 136712. [\[CrossRef\]](#) [\[PubMed\]](#)
10. Xie, L.; Jiang, G.; Qian, F. Experimental Research on Aftertreatment SCR Sizing Strategy for a Nonroad Mid-Range Diesel Engine. *Energies* **2020**, *13*, 4462. [\[CrossRef\]](#)
11. Ciardelli, C.; Nova, I.; Tronconi, E.; Chatterjee, D.; Bandl-Konrad, B. A “Nitrate Route” for the low temperature “Fast SCR” reaction over a $\text{V}_2\text{O}_5\text{-WO}_3/\text{TiO}_2$ commercial catalyst. *Chem. Commun.* **2004**, *23*, 2718–2719. [\[CrossRef\]](#) [\[PubMed\]](#)

12. Yang, X.G.; Ma, Q.; Niu, G.P.; Xu, X.T. Effect of fast SCR reaction on denitration characteristics of commercial V_2O_5 - WO_3 / TiO_2 catalysts. *Chin. J. Environ. Eng.* **2018**, *12*, 1968–1976.
13. Yao, D.W.; Liu, B.A.; Wu, F.; Li, Y.X.; Hu, X.H.; Jin, W.Y.; Wang, X.L. N_2O Formation Mechanism During Low-Temperature NH_3 -SCR over Cu-SSZ-13 Catalysts with Different Cu Loadings. *Ind. Eng. Chem. Res.* **2021**, *60*, 10083–10093. [\[CrossRef\]](#)
14. Kim, M.H.; Park, S.W. Selective reduction of NO by NH_3 over Fe-zeolite-promoted V_2O_5 - WO_3 / TiO_2 -based catalysts: Great suppression of N_2O formation and origin of NO removal activity loss. *Catal. Commun.* **2016**, *86*, 82–85. [\[CrossRef\]](#)
15. Sharp, C.; Zavala, B.; Neely, G.; Rao, S. *An Update on Continuing Progress towards Heavy-Duty Low NO_x and CO_2 in 2027 and Beyond*; No. 2023-01-0357; SAE Technical Paper: Warrendale, PA, USA, 2023. [\[CrossRef\]](#)
16. Imdadul, H.K.; Masjuki, H.H.; Kalam, M.A.; Zulkifli, N.W.M.; Alabdulkarem, A.; Rashed, M.M.; Teoh, Y.H.; How, H.G. Higher alcohol–biodiesel–diesel blends: An approach for improving the performance, emission, and combustion of a light-duty diesel engine. *Energy Convers. Manag.* **2016**, *111*, 174–185. [\[CrossRef\]](#)
17. Jung, Y.J.; Pyo, Y.; Jang, J.; Woo, Y.; Ko, A.; Kim, G.; Shin, Y.; Cho, C. Nitrous oxide in diesel aftertreatment systems including DOC, DPF and urea-SCR. *Fuel* **2021**, *310*, 122453. [\[CrossRef\]](#)
18. Jiao, P.H.; Li, Z.J.; Shen, B.X.; Zhang, W.; Kong, X.J.; Jiang, R. Research of DPF regeneration with NO_x -PM coupled chemical reaction. *Appl. Therm. Eng.* **2017**, *110*, 737–745. [\[CrossRef\]](#)
19. Bai, S.Z.; Tang, J.; Wang, G.H.; Li, G.X. Soot loading estimation model and passive regeneration characteristics of DPF system for heavy-duty engine. *Appl. Therm. Eng.* **2016**, *100*, 1292–1298. [\[CrossRef\]](#)
20. Nova, I.; Ciardelli, C.; Tronconi, E.; Chatterjee, D.; Weibel, M. Unifying Redox Kinetics for Standard and Fast NH_3 -SCR over a V_2O_5 - WO_3 / TiO_2 Catalyst. *AIChE J.* **2009**, *55*, 1514–1529. [\[CrossRef\]](#)
21. Bai, S.Z.; Han, J.L.; Liu, M.; Qin, S.S.; Wang, G.H.; Li, G.X. Experimental investigation of exhaust thermal management on NO_x emissions of heavy-duty diesel engine under the world Harmonized transient cycle (WHTC). *Appl. Therm. Eng.* **2018**, *142*, 421–432. [\[CrossRef\]](#)
22. Li, Y.; Zhu, Y.; Zhang, N.; Liu, Z. Simulation of Denitrification of Vehicle Exhaust over Cu-CHA Bazite Catalyst for a Monolith Reactor. *Catalysts* **2021**, *11*, 930. [\[CrossRef\]](#)
23. Liu, B.; Yao, D.W.; Wu, F.; Wei, L.; Li, X.W.; Wang, X.L. Experimental Investigation on N_2O Formation during the Selective Catalytic Reduction of NO_x with NH_3 over Cu-SSZ-13. *Ind. Eng. Chem. Res.* **2019**, *58*, 20516–20527. [\[CrossRef\]](#)
24. Hsieh, M.F.; Wang, J.M. NO and NO_2 Concentration Modeling and Observer-Based Estimation Across a Diesel Engine Aftertreatment System. *J. Dyn. Syst. Meas. Control Trans. ASME* **2011**, *133*, 041005. [\[CrossRef\]](#)

Disclaimer/Publisher’s Note: The statements, opinions and data contained in all publications are solely those of the individual author(s) and contributor(s) and not of MDPI and/or the editor(s). MDPI and/or the editor(s) disclaim responsibility for any injury to people or property resulting from any ideas, methods, instructions or products referred to in the content.